

Electrical and Optical Properties of Layered Oxysulfides with CuS Layers: Sr–Cu–M–O–S System (M = Zn, Ga, In)

K. Ueda,^{*,†} S. Hirose,[†] H. Kawazoe,[‡] and H. Hosono[†]

Materials and Structures Laboratory, Tokyo Institute of Technology, 4259, Nagatsuta, Midori, Yokohama, 226-8503, Japan, and R&D Center, HOYA Company, 3-3-1 Musashino, Akishima 196-8510, Japan

Received September 28, 2000. Revised Manuscript Received March 2, 2001

The electrical and optical properties of layered oxysulfides (Sr–Cu–M–O–S system (M = Zn, Ga, In)), which have common CuS layers, were studied to examine their potential as wide-gap p-type semiconductors. The attempts of electrical conductivity control by Na doping demonstrated that the conductivities of the $\text{Sr}_{2-x}\text{Na}_x\text{Cu}_2\text{ZnO}_2\text{S}_2$ ($\sigma = 2.2 \times 10^{-8} \text{ S cm}^{-1}$ for $x = 0.0$) and $\text{Sr}_{2-x}\text{Na}_x\text{CuGaO}_3\text{S}$ ($\sigma = 2.2 \times 10^{-4} \text{ S cm}^{-1}$ for $x = 0.0$) at room temperature increased up to 1.2×10^{-1} and $2.4 \times 10^{-2} \text{ S cm}^{-1}$ for $x = 0.1$, respectively, with an increase in Na concentration. In addition, both Hall and Seebeck measurements proved that these conductive oxysulfides were p-type semiconductors. The diffuse reflectance spectra of the materials revealed that the optical absorption edges were approximately 450 nm for $\text{Sr}_2\text{Cu}_2\text{ZnO}_2\text{S}_2$, 480 nm for $\text{Sr}_2\text{CuGaO}_3\text{S}$, and 540 nm for $\text{Sr}_2\text{CuInO}_3\text{S}$. It became evident from these results that the layered oxysulfides (Sr–Cu–M–O–S system (M = Zn, Ga, In)) were wide-gap p-type semiconductors utilizing the CuS layers as electrical conduction paths.

Introduction

Tin-doped indium oxide (ITO) and aluminum-doped zinc oxide (AZO) are well-known as transparent conductive oxides (TCOs) and used in a variety of technological applications. Although these materials can be regarded as semiconductors with large energy gaps, their use is limited to transparent conducting contacts in flat-panel displays or solar cells just because of their n-type monopolarity in the electrical conduction. Therefore, p-type TCOs are considered as key materials that enable a new class of p–n junction-based devices with transparent character.

Some p-type TCOs, CuMO_2 (M = Al, Ga, In)^{1–5} and SrCu_2O_2 ,⁶ were recently found on the basis of our material design. Moreover, our development of transparent p-type semiconductors has been extended successfully to a layered oxysulfide of LaCuOS .^{7,8} The essence of our material design is the modulation of the top of the valence band, which is generally composed of

highly electronegative oxygen 2p⁶ bands in typical wide-gap oxides. The modulation is carried out by mixing of the oxygen 2p⁶ bands with copper 3d¹⁰ and sulfur 3p⁶ bands to reduce the large electronegativity of the oxygen 2p⁶ bands.

In the exploration for other wide-gap p-type conductive materials, we noted some layered oxysulfides in the Sr–Cu–M–O–S system (M = Zn, Ga, In) reported by W. J. Zhu and P. H. Hor.^{9–12} Figure 1 shows the crystal structures of $\text{Sr}_2\text{Cu}_2\text{ZnO}_2\text{S}_2$ and $\text{Sr}_2\text{CuMO}_3\text{S}$ (M = Ga, In). These oxysulfides consist of four types of layers along the *c*-axis: SrO oxide layer, MO (M = Zn, Ga, In) oxide layer, CuS sulfide layer, and Sr²⁺ cation layer. The CuS layer, which is seen in some chalcogenides,^{13–15} is visualized as an anti-PbO-type sheet composed of the edge-sharing CuS_4 tetrahedra. The tetrahedral environment around Cu⁺ manifests the strong covalence of Cu–S bonds in the CuS layers.¹⁶ This local structure gives a marked contrast to the linear O–Cu–O bonds in Cu⁺-containing oxides. These layered crystal structures are similar to the structure of LaCuOS and satisfy the requirements for wide-gap p-type conductive features as found in LaCuOS : the layered structure composed of the CuS layers intervened by highly ionic oxide layers. Therefore, $\text{Sr}_2\text{Cu}_2\text{ZnO}_2\text{S}_2$ and $\text{Sr}_2\text{CuMO}_3\text{S}$

* To whom correspondence should be addressed. E-mail: kueda1@rlem.titech.ac.jp.

[†] Tokyo Institute of Technology.

[‡] HOYA Co.

(1) Kawazoe, H.; Yasukawa, M.; Hyodo, H.; Kurita, M.; Yanagi, H.; Hosono, H. *Nature* **1997**, *389*, 939.

(2) Yanagi, H.; Inoue, S.; Ueda, K.; Kawazoe, H.; Hosono, H. *J. Appl. Phys.* **2000**, *88*, 4159.

(3) Yanagi, H.; Kudo, A.; Ueda, K.; Hosono, H.; Kawazoe, H. *J. Electroceram.* **2000**, *4*, 427.

(4) Ueda, K.; Hase, T.; Yanagi, H.; Kawazoe, H.; Hosono, H.; Orita, M.; Hirano, M. *J. Appl. Phys.* **2001**, *89*, 1790.

(5) Yanagi, H.; Hase, T.; Ibuki, S.; Ueda, K.; Hosono, H. *Appl. Phys. Lett.* **2001**, *78*, 1583.

(6) Kudo, A.; Yanagi, H.; Hosono, H.; Kawazoe, H. *Appl. Phys. Lett.* **1998**, *73*, 220.

(7) Ueda, K.; Inoue, S.; Hirose, S.; Kawazoe, H.; Hosono, H. *Appl. Phys. Lett.* **2000**, *77*, 2701.

(8) Ueda, K.; Inoue, S.; Hosono, H.; Sarukura, N.; Hirano, M. *Appl. Phys. Lett.* **2001**, *78*, 2333.

(9) Zhu, W. J.; Hor, P. H. *Inorg. Chem.* **1997**, *36*, 357.

(10) Zhu, W. J.; Hor, P. H. *J. Solid State Chem.* **1997**, *130*, 319.

(11) Zhu, W. J.; Hor, P. H. *J. Solid State Chem.* **1997**, *134*, 128.

(12) Zhu, W. J.; Hor, P. H. *J. Am. Chem. Soc.* **1997**, *119*, 12398.

(13) Saeki, M.; Onoda, M.; Nozaki, H. *Mater. Res. Bull.* **1988**, *23*, 603.

(14) Palazzi, M.; Carcaly, C.; Flahaut, J. *J. Solid State Chem.* **1980**, *35*, 159.

(15) Park, Y.; DeGroot, D. C.; Schindler, J. L.; Kannewurf, C. R.; Kanatzidis, M. G. *Chem. Mater.* **1993**, *5*, 8.

(16) Ouammou, A.; Mouallem-Bahout, M.; Peña, O.; Halet, J.; Saillard, J.; Claude, C. *J. Solid State Chem.* **1995**, *117*, 73.

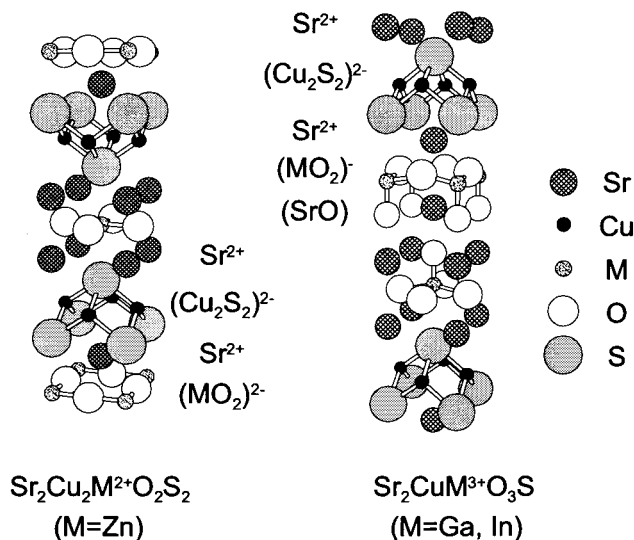


Figure 1. Crystal structures of $\text{Sr}_2\text{Cu}_2\text{ZnO}_2\text{S}_2$ and $\text{Sr}_2\text{-CuMO}_3\text{S}$ (M = Ga, In).

(M = Ga, In) seem to be fairly promising as wide-gap p-type semiconductors. Besides, Ga, In, and Zn oxide layers in these oxysulfides imply a possibility of n-type conduction because these monoxides are well-known as n-type TCOs.

Although the crystal structure of the oxysulfides in the Sr–Cu–M–O–S system were well examined by W. J. Zhu and P. H. Hor, no electrical and optical properties of these materials have been reported yet. In this paper, the electrical properties, especially the control of the electrical conductivities of $\text{Sr}_2\text{Cu}_2\text{ZnO}_2\text{S}_2$ and $\text{Sr}_2\text{-CuMO}_3\text{S}$ (M = Ga, In) by cation doping, as well as their optical properties are examined to estimate their potential as optoelectronic materials.

Experimental Section

Sample Preparation. $\text{Sr}_{2-x}\text{Na}_x\text{Cu}_2\text{ZnO}_2\text{S}_2$. Stoichiometric amounts of SrS, Cu_2O , Na_2S , and ZnO powders were thoroughly mixed in a mortar and pressed into pellets. The pellets were calcined at 920 °C in an Ar flow for 4 h. After the pellets were ground and the powders were molded into the pellets with a cold isostatic press, the pellets were sintered at 870 °C in an Ar flow for 3 h.

$\text{Sr}_{2-x}\text{Na}_x\text{CuGaO}_3\text{S}$. $\text{Sr}_3\text{Ga}_2\text{O}_6$ was first prepared by reacting SrCO_3 and Ga_2O_3 at 1050 °C in O_2 flow for 12 h. The starting materials of SrS, Cu_2O , Ga_2O_3 , Na_2S , and $\text{Sr}_3\text{Ga}_2\text{O}_6$ were stoichiometrically mixed in a mortar. The mixed powders were pressed into pellets and placed in a tungsten crucible. The crucible was heated to 850 °C in an Ar atmosphere of 500 Torr for 4 h using a microwave induction heater. The samples were obtained by regrinding the pellets, pelletizing the powders with a cold isostatic press, and heating the tungsten crucible with the pellets in the same condition above.

$\text{Sr}_2\text{CuInO}_3\text{S}$. $\text{Sr}_2\text{CuInO}_3\text{S}$ was prepared from stoichiometric amounts of SrS, Cu_2O , SrO, and In_2O_3 . SrO was obtained by firing SrCO_3 at 1200 °C. Using these mixed powders, the sintered pellets of $\text{Sr}_2\text{CuInO}_3\text{S}$ were obtained through the same procedures as $\text{Sr}_2\text{CuGaO}_3\text{S}$.

Characterization. Chemical compositions of the samples were examined by inductively coupled plasma emission spectroscopy (ICP). X-ray diffraction (XRD) patterns were measured to confirm a single phase of each sample and to refine the lattice constants of the materials by the least-squares method.

The electrical conductivities of the samples were measured from 300 to 10 K by the two-probe technique for slightly

Table 1. Cation Ratios Analyzed by the ICP Method

sample	Sr	Cu	M (M = Zn, Ga, In)	Na
$\text{Sr}_2\text{Cu}_2\text{ZnO}_2\text{S}_2$	2.00	2.04	0.98	
$\text{Sr}_{1.9}\text{Na}_{0.1}\text{Cu}_2\text{ZnO}_2\text{S}_2$	1.90	1.98	0.99	0.11
$\text{Sr}_2\text{CuGaO}_3\text{S}$	2.00	0.97	1.02	
$\text{Sr}_{1.9}\text{Na}_{0.1}\text{CuGaO}_3\text{S}$	1.90	1.01	0.97	0.09
$\text{Sr}_2\text{CuInO}_3\text{S}$	2.00	0.99	1.04	

conductive samples or the four-probe technique for highly conductive samples. Au electrodes were sputtered on the surfaces of the samples, and the measurements were carried out after confirming their ohmic contact.

Hall and Seebeck coefficients of $\text{Sr}_{1.9}\text{Na}_{0.1}\text{Cu}_2\text{ZnO}_2\text{S}_2$ and $\text{Sr}_{1.9}\text{Na}_{0.1}\text{CuGaO}_3\text{S}$ samples were measured at room temperature. The Hall measurements were performed by the Van der Pauw method under the magnetic field of 0.7 T.

The diffuse reflectance spectra of powdered samples were measured in the visible and near-infrared region using a spectrophotometer with an integrating sphere.

Results and Discussion

Chemical compositions of the samples analyzed by the ICP method are summarized in Table 1. The chemical analysis clarified that the cation ratios of the samples almost agreed with the nominal compositions. The XRD patterns of the nondoped samples revealed that each sample was a single phase: all diffraction peaks in the patterns were completely indexed on the basis of the crystal structure reported by W. J. Zhu and P. H. Hor.^{9–12} The Na-doped samples gave almost the same patterns as the nondoped samples. Their lattice constants refined by the least-squares method are listed in Table 2. In each nondoped sample, the lattice constant *a* was in good agreement with that reported by W. J. Zhu and P. H. Hor, while *c* was a little larger than the reported data. The colors of the samples and the densities of the sintered pellets are listed in Table 3.

The maximum solubility of Na^+ , which substitutes for Sr^{2+} as an acceptor, was found to be $x \sim 0.10$ in both $\text{Sr}_{2-x}\text{Na}_x\text{Cu}_2\text{ZnO}_2\text{S}_2$ and $\text{Sr}_{2-x}\text{Na}_x\text{CuGaO}_3\text{S}$. In the attempt of Na doping into $\text{Sr}_2\text{CuInO}_3\text{S}$, the single-phase sample could not be obtained by the present preparatory method. The difference in lattice constants between the nondoped and Na-doped samples was fairly small as shown in Table 2. This is probably because the size of a Na^+ ion (1.18 Å) is close to that of a Sr^{2+} ion (1.26 Å) and the amount of the substitution is not sufficient to cause the difference in lattice constants.

Figure 2a,b show the electrical conductivities of $\text{Sr}_{2-x}\text{Na}_x\text{Cu}_2\text{ZnO}_2\text{S}_2$ and $\text{Sr}_{2-x}\text{Na}_x\text{CuGaO}_3\text{S}$ as a function of temperature, respectively. In Figure 2a, the nondoped $\text{Sr}_2\text{Cu}_2\text{ZnO}_2\text{S}_2$ sample showed the electrical conductivity as low as $\sim 2.2 \times 10^{-8} \text{ S cm}^{-1}$ at room temperature. As the concentration of Na^+ increased, the electrical conductivity of $\text{Sr}_{2-x}\text{Na}_x\text{Cu}_2\text{ZnO}_2\text{S}_2$ drastically increased. The electrical conductivity of the $x = 0.10$ sample at room temperature was $1.2 \times 10^{-1} \text{ S cm}^{-1}$, which is larger than that of the nondoped sample by 7 orders of magnitude. The temperature dependence of the conductivity of $\text{Sr}_{2-x}\text{Na}_x\text{Cu}_2\text{ZnO}_2\text{S}_2$ showed semiconducting behavior in small *x* and degenerated-semiconducting behavior in $x = 0.06$ and 0.10 at low temperatures.

The electrical conductivity of nondoped $\text{Sr}_2\text{CuGaO}_3\text{S}$ was $\sim 2.2 \times 10^{-4} \text{ S cm}^{-1}$ at room temperature as seen in Figure 2b. The electrical conductivity of the nondoped

Table 2. Lattice Constants Refined by the Least-Squares Method^a

sample	<i>a</i> (Å)	σ_a^b	<i>c</i> (Å)	σ_c^b
Sr ₂ Cu ₂ ZnO ₂ S ₂	4.007 (4.008)	2.877×10^{-4}	17.736 (17.720)	1.533×10^{-3}
Sr _{1.9} Na _{0.1} Cu ₂ ZnO ₂ S ₂	4.009	4.882×10^{-4}	17.740	2.138×10^{-3}
Sr ₂ CuGaO ₃ S	3.864 (3.861)	7.582×10^{-5}	15.755 (15.730)	3.872×10^{-4}
Sr _{1.9} Na _{0.1} CuGaO ₃ S	3.865	1.290×10^{-4}	15.755	6.538×10^{-4}
Sr ₂ CuInO ₃ S	4.094 (4.091)	1.369×10^{-4}	15.530 (15.473)	6.109×10^{-4}

^a Data by W. J. Zhu and P. H. Hor⁹⁻¹² are listed in parentheses. ^b Standard deviation.

Table 3. Electrical and Optical Properties of Samples at Room Temperature

sample	color	pellet density (%)	conductivity (S cm ⁻¹)	Seebeck coefficient (μV K ⁻¹)	Hall constant (cm ³ C ⁻¹)	absorption edge (nm)
Sr ₂ Cu ₂ ZnO ₂ S ₂	pale yellow	85	2.2×10^{-8}			450
Sr _{1.9} Na _{0.1} Cu ₂ ZnO ₂ S ₂	olive	92	1.2×10^{-1}	+310	+6.7	450
Sr ₂ CuGaO ₃ S	yellow	72	2.2×10^{-4}			480
Sr _{1.9} Na _{0.1} CuGaO ₃ S	green	82	2.4×10^{-2}	+460		480
Sr ₂ CuInO ₃ S	orange	72	2.2×10^{-10}			540

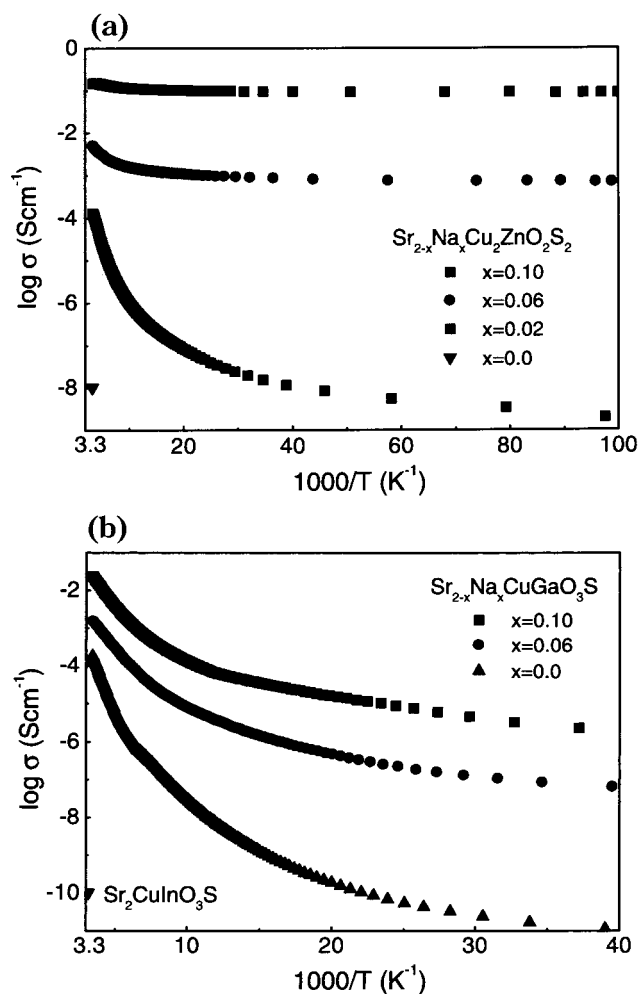


Figure 2. Electrical conductivities of (a) Sr_{2-x}Na_xCu₂ZnO₂S₂ and (b) Sr_{2-x}Na_xCuGaO₃S as a function of temperature. The electrical conductivity of Sr₂CuInO₃S at room temperature is plotted in Figure 2b.

sample probably resulted from carrier generation by a small amount of Cu⁺ vacancies that was not clearly detected by ICP. The temperature dependence of the conductivity of Sr_{2-x}Na_xCuGaO₃S samples showed the semiconducting behavior up to *x* = 0.10. The electrical conductivity of the *x* = 0.10 sample was $\sim 2.4 \times 10^{-2}$ S cm⁻¹ at room temperature. Sr₂CuInO₃S was almost insulating, and its electrical conductivity at room temperature was $\sim 2.2 \times 10^{-10}$ S cm⁻¹, as plotted in Figure 2b.

These results on the electrical conductivity revealed that acceptor doping by Na⁺ substitution for Sr²⁺ is fairly effective in both Sr_{2-x}Na_xCu₂ZnO₂S₂ and Sr_{2-x}Na_xCuGaO₃S, and the electrical conductivity can be controlled from insulating to semiconducting by Na⁺ concentration. We also tried donor doping as well as acceptor doping in SrCu₂ZnO₂S₂ and Sr₂CuInO₃S: La or Y substitution for Sr, Al or Ga substitution for Zn, and Sn substitution for In. However, no remarkable change in the electrical conductivity was observed, and these trials were unsuccessful in the present study. Because the formation of Cu⁺ vacancies frequently occurs in these oxysulfides, carrier compensation seems to occur in the donor-doped materials.

The Seebeck measurements were carried out using highly conductive samples of *x* = 0.10. The Seebeck coefficients of Sr_{1.9}Na_{0.1}Cu₂ZnO₂S₂ and Sr_{1.9}Na_{0.1}CuGaO₃S were +310 μV K⁻¹ and +460 μV K⁻¹, respectively. The Hall measurement was successful only for Sr_{1.9}Na_{0.1}Cu₂ZnO₂S₂ and its Hall coefficient was +6.7 cm³ C⁻¹. The positive sign of the Seebeck and Hall coefficients confirmed that these oxysulfides are p-type semiconductors and Na⁺ ions at Sr²⁺ ion sites actually act as acceptors. These results on the electrical transport properties are listed in Table 3. The carrier density and Hall mobility of Sr_{1.9}Na_{0.1}Cu₂ZnO₂S₂ were evaluated to be 1.1×10^{18} cm⁻³ and 0.74 cm² V⁻¹ s⁻¹. The yield of the hole carriers was estimated to be 0.3% on the assumption that each Na⁺ ion generates a single positive hole. This indicates that only a small portion of Na⁺ ions act as acceptors.

Figure 3a shows the diffuse reflectance spectra of Sr₂Cu₂ZnO₂S₂, Sr₂CuGaO₃S, and Sr₂CuInO₃S. The diffuse reflectance drops to the minimum at ~ 450 nm for Sr₂Cu₂ZnO₂S₂, ~ 480 nm for Sr₂CuGaO₃S, and ~ 540 nm for Sr₂CuInO₃S. Because the diffuse reflectance is generally regarded as the transmittance through the small crystals of samples, the drop of the diffuse reflectance is considered as the fundamental absorption edge of the samples in a first approximation. Accordingly, it was found from the spectra that these oxysulfides have relatively wide energy gaps and Sr₂Cu₂ZnO₂S₂ has the largest energy gap (~ 2.7 eV) among them. However, the energy gap of these oxysulfides was not as large as that of LaCuOS, probably because of the dispersion of the conduction band primarily composed of the Zn 4s, Ga 4s, or In 5s band.

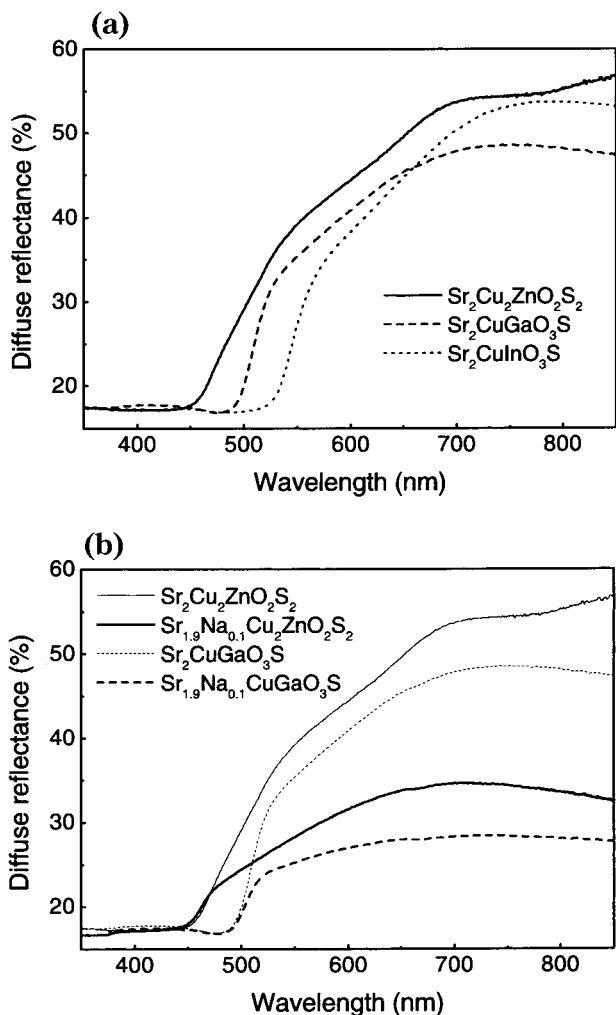
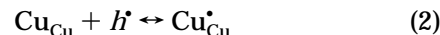
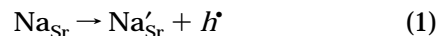


Figure 3. Diffuse reflectance spectra of (a) $\text{Sr}_2\text{Cu}_2\text{ZnO}_2\text{S}_2$ (solid line), $\text{Sr}_2\text{CuGaO}_3\text{S}$ (dashed line), and $\text{Sr}_2\text{CuInO}_3\text{S}$ (dotted line) and (b) $\text{Sr}_{1.9}\text{Na}_{0.1}\text{Cu}_2\text{ZnO}_2\text{S}_2$ (thick solid line) and $\text{Sr}_{1.9}\text{Na}_{0.1}\text{CuGaO}_3\text{S}$ (thick dashed line).

Figure 3b shows the diffuse reflectance spectra of $\text{Sr}_{1.9}\text{Na}_{0.1}\text{Cu}_2\text{ZnO}_2\text{S}_2$ and $\text{Sr}_{1.9}\text{Na}_{0.1}\text{CuGaO}_3\text{S}$ along with their nondoped samples. The drop of the diffuse reflectance of the Na-doped samples occurs at the same wavelength as that of the nondoped samples. This indicates that the Na^+ substitution for Sr^{2+} does not have a significant influence on the electronic structure of the materials. However, the reflectance of the Na-doped samples in the visible to infrared region largely decreased in comparison with that of the nondoped samples. This reflectance decrease is related to the presence of a small amount of Cu^{2+} , which was generated by Na doping, and caused the change in the color of the samples as listed in Table 3.

It is well-known that mixed valence copper compounds usually show broad absorption in the visible to infrared range because of the d-d transition in Cu^{2+} ions and the charge transfer between Cu^+ and Cu^{2+}

ions.^{17,18} The origin of the reflectance decrease observed in $\text{Sr}_{2-x}\text{Na}_x\text{Cu}_2\text{ZnO}_2\text{S}_2$ and $\text{Sr}_{2-x}\text{Na}_x\text{CuGaO}_3\text{S}$ is considered to be the optical absorption originating from the mixed valence of the copper ions. The electrical and optical properties in the Na-doped samples are explained by the following two reactions expressed by Kröger-Vink notation.¹⁹



Reaction (1) expresses the ionization of Na^+ ions at Sr^{2+} ion sites accompanying the generation of positive holes in the valence band. On the other hand, reaction (2) represents the charge transfer between Cu^+ (Cu_{Cu}) and Cu^{2+} (Cu^*_{Cu}), which occurs primarily within each CuS layer. This reaction is responsible for the mixed valence absorption and p-type electrical conduction. Therefore, it is interpreted that Cu 3d bands largely contribute to the top of the valence band in the Sr-Cu-M-O-S oxysulfides ($M = \text{Zn, Ga, In}$) and the CuS layers in these materials can be visualized as conduction paths for positive holes.

Conclusion

A single phase of an oxysulfide with CuS layers, $\text{Sr}_2\text{Cu}_2\text{ZnO}_2\text{S}_2$, $\text{Sr}_2\text{CuGaO}_3\text{S}$, or $\text{Sr}_2\text{CuInO}_3\text{S}$, was successfully prepared to examine its electrical and optical properties. The nondoped $\text{Sr}_2\text{Cu}_2\text{ZnO}_2\text{S}_2$ and $\text{Sr}_2\text{CuInO}_3\text{S}$ were almost insulating, while the nondoped $\text{Sr}_2\text{CuGaO}_3\text{S}$ was semiconducting at room temperature. Although Na doping was unsuccessful against $\text{Sr}_2\text{CuInO}_3\text{S}$, the electrical conductivity of Na-doped samples, $\text{Sr}_{2-x}\text{Na}_x\text{Cu}_2\text{ZnO}_2\text{S}_2$ and $\text{Sr}_{2-x}\text{Na}_x\text{CuGaO}_3\text{S}$, increased with an increase in Na concentration. Both Seebeck and Hall measurements revealed that the Na-doped conductive materials were p-type semiconductors. Therefore, acceptor doping by Na^+ substitution for Sr^{2+} was found to be effective in controlling their electrical conductivities. On the other hand, the conductivity control by donor doping in each material was unsuccessful in the present study. The diffuse reflectance spectra of these materials indicated that the materials have relatively wide energy gaps and $\text{Sr}_2\text{Cu}_2\text{ZnO}_2\text{S}_2$ has the largest energy gap among them. The change in the reflectance spectra and the electrical conduction of the Na-doped samples was discussed in terms of the mixed valence states of Cu^+ and Cu^{2+} ions. According to these results, the p-type electrical conductive and wide-gap character was found in the layered oxysulfides (Sr-Cu-M-O-S system ($M = \text{Zn, Ga, In}$)) with CuS layers.

CM0007813

(17) Robin, M. B.; Day, P. *Adv. Inorg. Chem. Radiochem.* **1967**, *10*, 247.

(18) Sigwart, C.; Hemmerich, P.; Spence, J. T. *Inorg. Chem.* **1968**, *7*, 2545.

(19) Kröger, F. A.; Vink, V. J. *Solid State Phys.* **1956**, *3*, 307.